Available online at www.sciencedirect.com
SCIENCE DIRECT
Journal of Photochemistry and Photobiology A: Chemistry 179 (2006) 305–313
Journal of Photochemistry and Photobiology A:Chemistry
www.elsevier.com/locate/jphotochem

Photoelectrochemical characterisation of TiO_2 thin films derived from microwave hydrothermally processed nanocrystalline colloids

Shanqing Zhang [a,*], William Wen [a], Dianlu Jiang [a], Huijun Zhao [a], Richard John [a], Gregory J. Wilson [b], Geoffrey D. Will [b]

[a] *Centre of Aquatic Processes and Pollution and School of Environmental and Applied Sciences, Griffith University, Gold Coast Campus, PMB 50, Gold Coast Mail Centre, Qld 9726, Australia*
[b] *Inorganic Materials Research Program, Queensland University of Technology, GPO Box 2434, Brisbane, Qld 4001, Australia*

Received 22 May 2005; received in revised form 1 August 2005; accepted 29 August 2005
Available online 28 September 2005

Abstract

Titanium dioxide (TiO_2) thin films fabricated with different TiO_2 colloids were characterised using photoelectrochemical techniques. TiO_2 colloids were firstly prepared via hydrolysis of titanium butoxide and peptisation process with no hydrothermal process (labelled as NP). The resulting colloids were then subjected to different hydrothermal processes, i.e., 15-h convection hydrothermal (labelled as CH) treatment; 5-, 10- and 15-min microwave hydrothermal treatment (labelled as M5, M10 and M15, respectively). The colloids were used to prepare TiO_2 thin films on conducting indium-doped tin oxide (ITO) substrates (i.e., CH, M15, M10, M5 and NP electrodes, respectively) using a controlled dip-coating technique. The experimental results demonstrate that the oxidation capacities of the electrodes for water and glucose are in the order of CH > M15 > M10 > M5 > NP. In contrast, the oxidation capacities of the electrodes for potassium hydrogen phthalate (KHP) are in the order of M15 > M10 > CH. It was also found that the CH electrode could be easily poisoned by high concentration of KHP, while microwave-processed electrodes (M15, M10 and M5) are immune from the KHP poisoning. The results presented demonstrate that microwave hydrothermal processing is a promising alternative method to the traditional convection hydrothermal treatment of colloids that provides electrodes with increased photocatalytic properties for the oxidation processes of adsorption-based organic compounds, such as KHP.

Keywords: TiO_2 electrode; Photoelectrochemical oxidation; Microwave; Hydrothermal treatment

1. Introduction

The interest of titanium dioxide (TiO_2) films exceeds that of TiO_2 colloids in their photocatalytic applications [1]. TiO_2 films are widely used in sensors [2–4], solar cells [5], self-cleaning windows [6], electrochromic devices [7] and photoelectrochemical degradation of organic waste [2,4,8–10]. It is generally accepted that the properties of nanoporous electrodes depend on the properties of the colloids used to fabricate them: the size and shape of the colloids from which the electrodes are made determine the porosity and the surface area to thickness ratio of the electrode [11]. One of the routine methods for preparing TiO_2 colloids is through sol–gel processing. This preparatory method has been exhaustively researched, since being instigated in the late 1800s. Refinements to the original methodology have focused on controlling the formation of crystalline phase during the hydrolysis stage and stability of the gels through modification of the colloidal precursors and peptising agents [12]. The quality of crystalline phases has also been shown to be greatly improved through post-hydrolysis hydrothermal treatment in a convection oven at moderately high temperatures (>200 °C) over sustained periods (up to 15 h).

Recently, we have reported efficient microwave hydrothermal preparation of nanocrystalline anatase TiO_2 colloids and its physiochemical characterisation using transmission electron microscopy (TEM), scanning electron microscopy (SEM), XRD, Raman spectrum and electron diffraction pattern techniques [13]. The results demonstrate that microwave hydrothermal treatment of colloidal TiO_2 gives comparable

* Corresponding author. Tel.: +61 7 5552 8155; fax: +61 7 5552 8067.
E-mail address: s.zhang@griffith.edu.au (S. Zhang).

1010-6030/$ – see front matter © 2005 Elsevier B.V. All rights reserved.
doi:10.1016/j.jphotochem.2005.08.034

increases in crystallinity with respect to traditional hydrothermal treatments, while requiring significantly less time and energy than the hydrothermal convection treatment [13]. Based on colloidal microwave processing, nanoscaled TiO_2 powders with properties improved over commercially available materials are obtained [14]. The resulting material displays the highest phase purity, narrowness of pore size distribution, accessibility of pores and photochemical activity among the materials tested. The main advantages identified were that the microwave hydrothermal process allowed for rapid heating to temperature and extremely rapid kinetics of crystallisation whilst retaining the desired properties of electronic materials [15].

Photoelectrochemistry is a powerful tool in its ability to evaluate the photoactivity of different TiO_2 nanocrystallites [16]. The immobilisation of TiO_2 on a conductive substrate permits potentiostatic control of thin nanocrystalline TiO_2 films, aiding charge separation of electrons in the bulk and holes at the surface. During the photoelectrochemical process, a photocurrent can be recorded and electrochemical techniques (e.g., amperometry, linear-sweep voltammetry) can be used to study the electron transfer at the semiconductor–solution interface.

In this work, different types of TiO_2 colloids (i.e., non-processed, microwave hydrothermally processed and conventional hydrothermally processed TiO_2 colloids) were immobilised on indium-doped tin oxide (ITO) conducting glass substrates, resulting in TiO_2 thin-film electrodes. The photoelectrochemical behaviour of the corresponding TiO_2 electrodes is presented. The electrochemical information obtained in the photoelectrochemical oxidation of glucose and potassium hydrogen phthalate (KHP) was used to evaluate the photoactivity forecasted by physicochemical properties of the TiO_2 crystallite: small particle size and high crystallinity. From a kinetic viewpoint, organic compounds can be classified into two defined groups in photocatalysis: those that are weakly adsorbed and those that are chemisorbed to the photocatalytic surface [17]. Glucose was chosen as a model compound as it represents a weakly adsorbed or non-adsorbed organic molecule, where the first step in the oxidation involves a bimolecular reaction with the formation of a trapped hole and a subsequent surface hydroxyl radical ($OH^{\bullet}$). Whilst KHP as a model compound represents a chemisorbed organic species, for which the initial step is direct photo-generated hole transferring to the surface complex [9,17].

2. Experimental

2.1. Materials

ITO conducting glass slides (8 Ω/square nominal resistivity) were commercially supplied by Delta Technologies Limited. Titanium butoxide (97%, Aldrich) and potassium hydrogen phthalate (AR, Aldrich) were used as received. All other chemicals were of analytical reagent grade and unless otherwise stated were purchased from Aldrich. All solutions were prepared using high purity deionised water (Millipore Corp., 18 MΩ cm).

2.2. Preparation of porous TiO_2 film electrodes

2.2.1. Preparation of colloidal TiO_2

Aqueous TiO_2 colloid was prepared by hydrolysis of titanium butoxide according to the method described by Barbe et al. [11]. Briefly, 16 cm^3 of isopropanol and 50 cm^3 of titanium butoxide were accurately measured into a 150 cm^3 dropping funnel. The resulting solution was added over 15 min with vigorous stirring to 600 cm^3 of Milli-Q water in a conical flask. On completion of the addition, 4.0 cm^3 of 70% nitric acid was added to the solution as a peptising agent. The conical flask containing the above solution was immersed in a hot water bath, heated to 80 °C and stirred continuously. After 10 h, approximately 400 cm^3 of a white colloidal solution remained and was stored in a darkened glass vessel. The sample, which was not further hydrothermally processed, was labelled as NP.

2.2.2. Convection hydrothermal (CH) treatment

A previously described procedure was followed to prepare convection hydrothermally treated titanium dioxide [5]. One hundred cubic centimetres of titania colloid prepared as above was placed into a 200 cm^3 Pyrex glass-lined stainless steel autoclave Parr-bomb. The sample was treated for 15 h at 200 °C in a convection oven (1300 W, SEM), cooled to room temperature for 2 h and the suspended product was allowed to stand for 24 h.

2.2.3. Microwave hydrothermal treatment

Microwave hydrothermal treatment has been reported in detail elsewhere [13]. Briefly, a 30 cm^3 aliquot of non-processed (NP) TiO_2 colloid was placed into a Teflon-lined digestion vessel. A microwave oven (1000 W, ETHOS MicroSYNTH microwave labstation, Milestone) was set at 80% power and the pressure ramped from atmospheric to the required pressure (60 psi) over a 2-min period. The duration of the treatment was 5, 10 and 15 min, with the resulting samples labelled as M5, M10 and M15, respectively.

2.2.4. Preparation of nanocrystalline TiO_2 thin-film electrodes

A measured volume of TiO_2 colloidal solution (NP, CH, M5, M10 or M15) prepared above was concentrated on a rotary evaporator to 8% (w/w) separately, a white semi-viscous colloidal solution resulting in. Forty percent TiO_2 weight equivalent (e.g., 1.6 g in 50 cm^3 8% colloidal solution) of polyethylene glycol Carbowax (6000 MW) was added to each resultant solution and stirred for approximately 20 min.

Films were prepared in a clean room environment to minimise contamination from dust particles. The TiO_2 colloidal solution was stirred vigorously and ultrasonicated for 20 min prior to dip-coating to achieve a consistent homogeneous mixture. The ITO slide was used as the electrode substrate and was pre-treated by washing in turn with detergent, water, acetone and water and finally dried by pure nitrogen gas. After pre-treatment, the ITO slide was dip-coated in the TiO_2 colloidal solution with a withdrawing speed of 1.0 cm/min. The coated electrodes were then calcined in a muffle furnace at 450 °C for 30 min in air. Double coating was achieved by repeating this procedure. The thickness

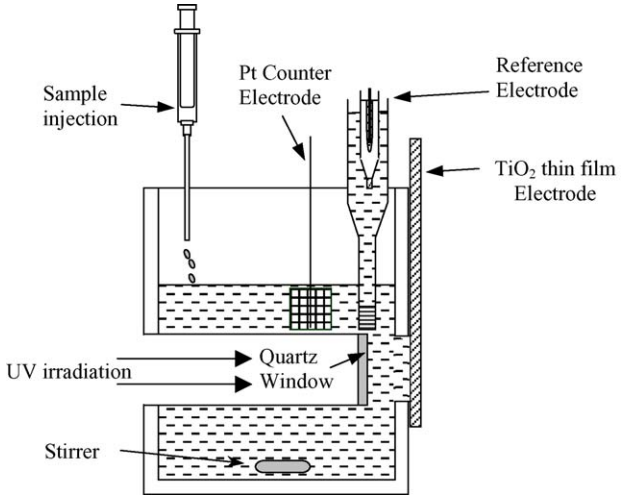

Fig. 1. Schematic diagram of the photoelectrochemical cell setup for the evaluation of TiO_2 thin-film electrodes. The distance between quartz window and working electrode is ~5 mm.

of the TiO_2 nanoporous film was 500–800 nm, measured with a surface profilometer (Alpha-step 200, Tencor Instruments).

2.2.5. *Electron micrographs of TiO_2 colloids and thin films*

The colloidal particles were immersion dispersed on a copper grid and the morphology and grain size of particles were determined using high resolution-transmission electron microscopy (HR-TEM) on the JEOL FX-2010F analytical scanning TEM operating at 200 kV.

Thin films prepared as above were scored on the reverse of the glass slide and broken to produce an edge profile for analysis. The film surface morphology and an estimate of the surface porosity were obtained using SEM on the JEOL JSM 6400 or the JEOL 840A analytical scanning SEM operating at 15 kV.

2.3. *Photoelectrochemical cell assembly and measurements*

All photoelectrochemical experiments were performed at 23 °C in a three-electrode electrochemical cell with a quartz window for illumination as shown in Fig. 1. The working electrode surface area exposed to solution was a circle with diameter of 10 mm. In order to minimise the absorption of UV light by the water solution, the distance between the quartz lens and working electrode was shortened to 6 mm by a Ø 14 mm quartz lens-fitted tube (see Fig. 1). Illumination was achieved with a 150 W xenon arc lamp light source with focusing lenses (HF-200w-95, Beijing Optical Instruments). To minimise sample heating from the infrared fraction of the source, the beam was passed through an UV-band pass filter (UG-5, Schott) prior to illuminating the electrode surface. Light intensity was 6.2 mW/cm^2, which was measured with a UV-irradiance meter (UVA, Instruments of Beijing Normal University). A saturated Ag/AgCl electrode and a platinum mesh were used as the reference and auxiliary electrodes, respectively, with 0.1 M $NaClO_4$ chosen as the supporting electrolyte. A voltammograph (CV-27, BAS) was used for application of potential bias in the photoelectrolysis and linear potential sweep experiments. Potential and current signals were recorded on a Macintosh computer (7220/200) coupled to a Maclab 400 interface (AD Instruments).

Table 1
Average crystallite sizes of TiO_2 colloids and TiO_2 films on electrodes calculated from XRD patterns

Sample	Particle size of TiO_2 colloid (nm)	Particle size of TiO_2 thin film (nm)
NP	3.4	6.2
M5	4.8	7.0
M10	4.8	9.5
M15	6.6	10.0
CH	10.2	12.6

3. Results and discussion

The colloids obtained from different processes, i.e., CH, M15, M10, M5 and NP, were characterised using XRD, TEM, Raman spectra and electron diffraction as described in the literature [13]. The results demonstrated that the CH processed and the microwave hydrothermally treated (M15, M10 and M5) TiO_2 samples were highly crystalline, while NP TiO_2 was semi-amorphous. The TiO_2 thin films that had been sintered at 450 °C for half an hour were also subjected to the XRD analysis. The result showed that the TiO_2 films were in agreement with the results attained for the colloids and consisted of primarily anatase with a very small amount of brookite phase present. This indicates that calcination at 450 °C does not change the crystalline phase of TiO_2. The average crystallite size of the TiO_2 colloid and those immobilised on the electrode were calculated using the Scherrer equation [13] and listed in Table 1. The convection hydrothermally processed colloid and its resulting electrode had the largest particle size due to the long hydrothermal process (i.e., 15 h), while the microwave-processed colloids also showed a proportional increase in crystallite size with treatment time. Accordingly, the non-hydrothermally processed samples had the smallest size. Comparatively, the nanocrystallite sizes of the TiO_2 electrode increased slightly over that of the colloidal form due to the calcination process at 450 °C with necking of particles and surface agglomeration leading to larger apparent sizes.

3.1. *Photoelectrochemical characterisation*

Under UV illumination, electrons in the TiO_2 semiconductor are promoted from the valence band to the conduction band. Positive charged holes remain in the valence band and electrons occupy the conduction band. TiO_2 electrodes prepared by immobilising TiO_2 on conducting substrates retain the photophysical and photochemical properties of individual particles and thus carry out the photocatalytic reactions with similar selectivity and efficiency as in TiO_2 suspensions [18]. Since the holes in the valence band can seize electrons, an appropriately irradiated TiO_2 electrode can serve as a photoanode to split water into oxygen and hydrogen [19,20] and oxidise a variety of organic pollutants in wastewater [18,21,22].

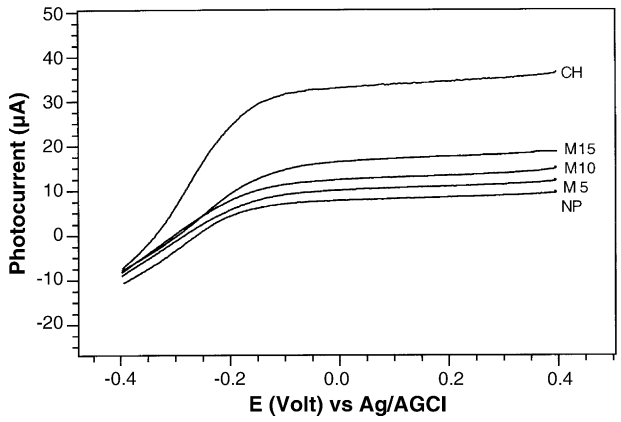

Fig. 2. Linear sweep voltammograms of TiO_2 electrodes at a scan rate of 10 mV/s in 0.1 M $NaClO_4$ solution under UV illumination. UV illumination intensity was 6.6 mW/cm^2.

Recombination of the induced electron–hole pair diminishes the photocatalytic activity of TiO_2 yet under a sufficiently positive potential, it has been shown that the recombination can be effectively inhibited [2]. Since effective separation of photo-generated electron–hole pairs occurs very close to the electrode–solution interface, it is of importance to concentrate on this region in our studies, since the rest of the electrode plays only the role of a conductor for the generated charge carriers. Under a given potential, thinner films favour an increased electrical field for the separation of electron–hole pair, hence, thinner films are more capable of realising charge separation over the whole layer of the TiO_2 thin film, leading to higher photocatalytic efficiency. Also thinner films have a smaller resistance compared with films of a greater thickness, which aids in the separation of electrons away from the site of excitation and hence the hole [23]. Thin films were therefore used to characterise the electrodes made from different colloids. The thickness of the electrode was controlled in the range of 500–800 nm by adjusting viscosity and withdrawing speed of the electrode from the coating solution during the preparation procedure.

In the absence of UV illumination, small negative currents were observed at potentials more negative than −0.30 V for all the TiO_2 electrodes. This is due to the TiO_2 crystallites not covering the entire surface of the conducting ITO substrate and the reduction of oxygen occurs at the naked ITO surface, generating negative currents under a sufficiently negative applied potential. Fig. 2 shows the voltammograms of the TiO_2 electrodes in 0.1 M $NaClO_4$ aqueous solution (pH 7) under UV illumination. As shown in Fig. 2, the negative currents for different TiO_2 electrodes maintained at the same magnitude at the negative potential under UV illumination, demonstrating that the reduction current is due to the electrochemical reduction of oxygen and is independent of the photoelectrochemical process.

Under UV illumination, the resulting photo-generated holes oxidise water molecules to produce a photocurrent. As shown in Fig. 2, the photocurrent increased with the applied potential before reaching a plateau. This photocurrent–potential characteristic is similar to that observed for TiO_2 single crystal electrodes [24]. The photocurrent becomes saturated when the applied potential is more positive than +0.2 V (versus Ag/AgCl reference). The applied potential was used for the harvesting of the electrons generated from the oxidation of water [25]. The saturated photocurrents observed at a potential >+0.20 V implies that the electrons generated from the oxidation of water molecules by valance holes were almost forced to transfer to the counter electrode via the electronic circuit. Therefore, further increase in applied potential would not result in a significant increase of the photocurrent. The sequence of the saturated photocurrent was in the order of CH > M15 > M10 > M5 > NP. The implication of this sequence is that in terms of water oxidation, the photoactivity of microwave hydrothermally processed colloids (M5, M10, M15) was significantly improved compared with the non-processed colloid, although they do not exhibit the same efficiency as the convection hydrothermally processed colloids. Also, the photocatalytic efficiency increased with the processing time of microwave hydrothermal treatment for the colloids, as indicated by the sequence of saturated photocurrents for the resulting electrodes in regard to water oxidation, i.e., M15 > M10 > M5.

3.2. Photoelectrochemical oxidation of glucose

In addition to the oxidation of water, organic compounds can also be oxidised at an illuminated TiO_2 electrode. In practice, organic compounds are more readily oxidised by the photoanode than water [26]. The photoelectrochemical oxidation of organic compounds is so effective that complete mineralisation of organic compound can be achieved with TiO_2 electrodes [2,25,27]. The general equation for mineralisation can be summarised as follows:

$$\begin{aligned} &C_yH_mO_jN_kX_q + (2y - j)H_2O \\ &\quad \rightarrow yCO_2 + qX^- + kNH_3 + (4y - 2j + m - 3k)H^+ \\ &\qquad + (4y - 2j + m - 3k - q)e^- \end{aligned} \quad (1)$$

where the elements present are represented by their atomic symbols and X represents a halogen atom. The stoichiometric ratio of elements in the organic compound is represented by the coefficients y, m, j, k and q.

Alcohols and aldehydes are readily oxidisable electrochemically but are more difficult to mineralise or oxidise completely to CO_2 due to the difficulty of decarboxylation, which requires carbon–carbon bond cleavage [28]. For example, the electrochemical oxidation of glucose to gluconic acid at a Pt electrode requires a very positive electrode (i.e., >+1.0 V versus SHE) [29]. In the absence of UV illumination, no significant Faraday current was observed for all the TiO_2 electrodes even when the glucose concentration was increased to 100 mM, which suggests that neither glucose nor water could be oxidised by the TiO_2 thin-film electrode at an applied potential of +0.30 V (versus Ag/AgCl).

A typical photocurrent response of TiO_2 thin-film electrode under UV illumination is presented in Fig. 3. As the figure indicates, a steady background current was first observed for the oxidation of water. With the injection of a higher glucose concentra-

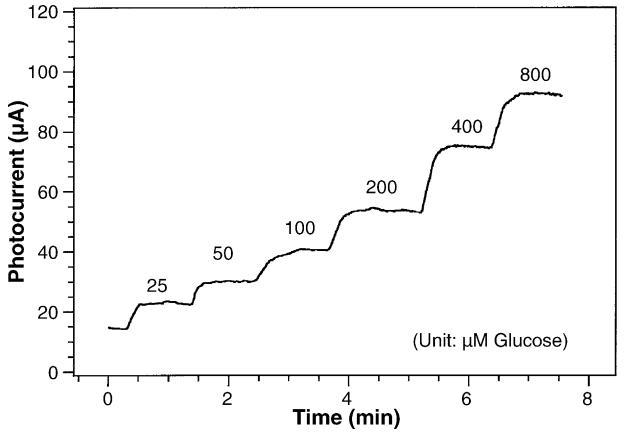

Fig. 3. Typical photocurrent response for the oxidation of glucose under constant stirring at −0.30 V vs. Ag/AgCl using a CH TiO_2 thin-film electrode. The concentration of glucose (μM) is indicated in the plateau region of the response. UV illumination intensity was 6.6 mW/cm^2.

tion, the photocurrent increases and then reaches a steady state, which is the aggregate current for the oxidation of water and glucose. Fig. 4 illustrates the photocurrents from different electrodes as a function of glucose concentration. The CH electrode had the highest background current and is dramatically higher than other electrodes (see Fig. 4a). The intensity of the background currents is in the order of CH > M15 > M10 > M5 > NP. This correlates to the order of the saturated current seen in the voltammograms in Fig. 2. The residual background current (when glucose concentration is zero) is also due to the oxidation of water [9], which is described in the previous section.

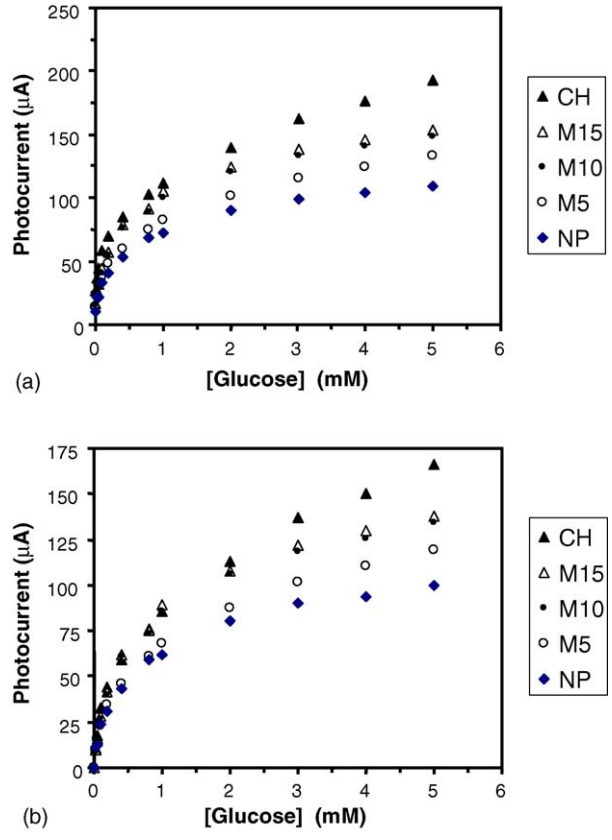

Fig. 4. (a and b) Photoelectrochemical oxidation of glucose using TiO_2 thin-film electrodes. Experimental conditions are as those indicated in Fig. 3.

Under UV illumination, the photocurrent increased with an increase in glucose concentration. The photocurrents indicated in Fig. 4a are the overall current for the oxidation of water and glucose. Comparatively, the water-splitting current was relatively stable even in the presence of different concentrations of organic compound [2]. In order to directly compare the oxidation ability with glucose, the background current due to the oxidation of water was subtracted from each overall current, respectively, and a new photocurrent profile as a function of glucose concentration was obtained and presented in Fig. 4b. The net photocurrent in Fig. 4b is a manifestation of the oxidation rate of the organic compound, glucose, in solution. Thus, the net current can be used to describe the oxidation capacity of the various TiO_2 electrode preparations. Fig. 4b clearly indicates that the sequence of increasing photocurrent was CH > M15 > M10 > M5 > NP. Therefore, the electrode made from non-processed colloid had the lowest oxidation ability while the electrode prepared from convection hydrothermal colloid had the strongest oxidation capacity in terms of glucose oxidation. Again, a trend is observed for the increase in microwave hydrothermal treatment time, with the oxidation ability of the resulting electrodes increasing with respect to treatment time.

As shown in Table 1, the order of the TiO_2 particle size was CH > M15 > M10 > M5 > NP. Smaller particle size normally results in an increase in exposed photocatalytic surface area; therefore, the order of the electrode surface area should be CH < M15 < M10 < M5 < NP, which is opposite to the trend of the photocurrent.

Under the same experimental conditions, besides surface area, crystallinity of the TiO_2 electrode can also affect the photocurrent. An explanation for the above anomaly, in the expected photocatalytic ability, can be found in the relative crystallinity of the particles, as it is well-known that crystallinity determines quantum efficiency [2] and becomes a significant property in the apparent oxidation ability. Poor crystallinity of the TiO_2 crystallite gives rise to low quantum efficiency. The XRD and electron diffraction data illustrated that the TiO_2 crystallites of the NP electrode had the lowest crystallinity, which was demonstrated in the literature [13]. Therefore, minimum quantum efficiency of NP electrodes can be attributed to lowest crystallinity of TiO_2 thin films that were made from the NP TiO_2 colloids. The converse is true, since as the degree of crystallinity increases in the microwave samples (M5 → M10 → M15), so does the apparent efficiency of the electrodes for glucose oxidation too, with the highly crystalline CH electrode having the highest oxidation efficiency in the studied electrodes. This rationalisation is supported by the proposed mechanism for oxidation of weakly adsorbed molecules at the titania surface. Highly crystalline materials will result in less defect sites due to the crystalline nature of the particles giving a surface rich in exposed Ti–O. The formation of $OH^{\bullet}$ radicals on the surface of TiO_2 occurs through weak adsorption of water molecules to the dangling bonds of oxygen atoms since the TiO_2 surface is slightly less saturated in comparison to the bulk. Under band gap excitation, positive charge carriers migrate

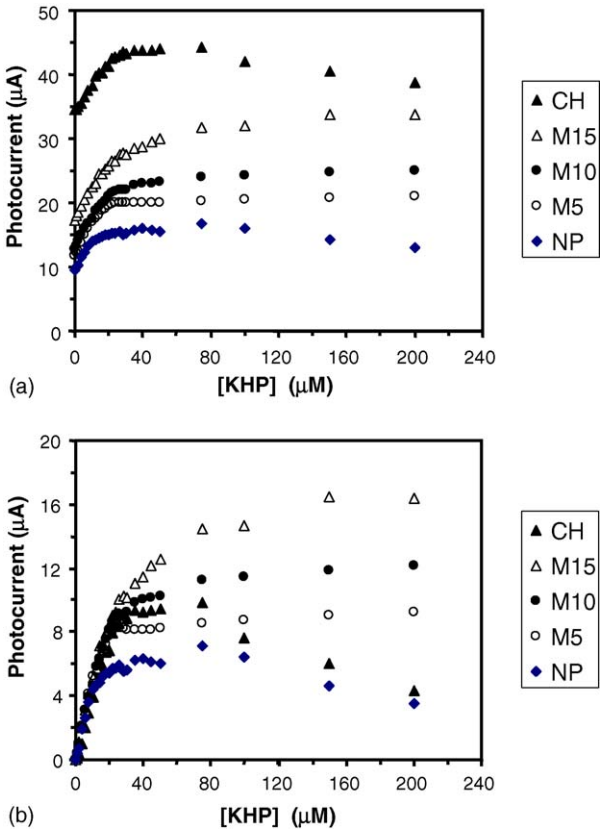

Fig. 5. (a and b) Photoelectrochemical oxidation of KHP using TiO_2 thin-film electrodes. Experimental conditions are as those indicated in Fig. 3.

to the surface resulting in $OH^{\bullet}$ radical formation. The increased crystalline material of the CH and microwave-processed electrodes leads to an increased concentration of surface hydroxyl radicals and hence a higher quantum efficiency for degradation of species oxidising via the weak adsorption mechanism.

3.3. Photoelectrochemical oxidation of KHP

The oxidation capacity of the TiO_2 electrodes for adsorbed organic compounds was also tested using KHP. Phthalic acid, the conjugate acid of KHP, is an aromatic compound having two carboxyl groups, which are known to strongly adsorb to the surface of TiO_2 [9]. Fig. 5a shows the photocurrent of TiO_2 thin-film electrodes as a function of KHP concentration, and Fig. 5b shows the net photocurrent resulting from the photoelectrochemical oxidation of KHP by subtracting the background current as described in Section 3.2. Fig. 5 is dramatically different from Fig. 4, due to the different oxidation mechanism that KHP undergoes in comparison to glucose as mentioned earlier. As was observed in Section 3.1 (Fig. 2), the background currents in Fig. 5a indicate that the rate of oxidation of water is affected by the method of treatment of colloidal precursors for the TiO_2 electrodes.

After subtraction of the background current (see Fig. 5b), the net photocurrents of all the TiO_2 electrodes were very similar at low KHP concentrations (<20 μM KHP). This demonstrated that all the TiO_2 photoanodes here are able to oxidise KHP, and suggested that under low concentration circumstances, the mass transport of KHP from the bulk solution to the electrode surface was the rate-limiting step among the interfacial processes.

In order to identify the oxidation capacity of the TiO_2 electrodes, the concentration of KHP was increased. When the KHP concentration was >20 μM, the difference in the photocurrent profiles begin to become significant. In the concentration range of 20–80 μM KHP, the photocurrents derived from the oxidation of KHP were in the order of M15 > M10 > CH > M5 > NP. The reasoning behind M5 TiO_2 electrode having a weaker KHP oxidation current than CH electrodes in this concentration range (Fig. 5b) is due principally to the insufficient photoactivity that results from inadequate microwave hydrothermal treatment, i.e., only 5 min. With extended treatment time, i.e., 10 and 15 min, M15 and M10 TiO_2 electrode demonstrated higher KHP oxidation current than CH electrodes.

Significant increase of the KHP oxidation currents for M15, M10 and M5 electrodes was not observed with any further increase of the KHP concentration (>80 μM KHP), which indicated that the KHP oxidation reaction had reached a limiting capacity for the M15, M10 and M5 electrodes. Interestingly, decreased overall photocurrents of the CH and NP electrodes were witnessed with increase of the KHP concentration (80–200 μM KHP). We identify this as a passivation effect, as a steady state current could be still obtained in this concentration range. With further increases in the KHP concentration (>250 μM), the overall photocurrent for CH and CP electrodes decreased even further, to a current, which was lower than their initial background currents, respectively. These photocurrents are not indicated in Fig. 5 because to obtain a steady state current it required a substantial deviation from the time scale in this scenario, i.e., the current keep decreasing to a very low current (e.g., <5 μA) over a very long time period (e.g., 1 h). This observation can be considered as poisoning of the CH and NP electrodes, as the electrodes not only lose their ability to efficiently oxidise KHP, but also diminish the ability to oxidise water. The reasons for surface poisoning of CH and NP electrodes are different. The apparent cause of the NP TiO_2 electrode poisoning can be attributed to the insufficient photoactivity due to the poor crystallinity as discussed previously, while the cause of the CH TiO_2 electrode poisoning will be discussed in detail below.

Of particular note in Fig. 5 is the reversal of the apparent oxidation capacity of the TiO_2 electrodes with the sequence of M15 > M10 > CH, in contrast to the situation of glucose oxidation in Fig. 4, where the sequence was CH > M15 > M10. This reversal can be reasonably explained with consideration of the relative porosity of the TiO_2 particles produced from the different hydrothermal processes and the mesoporous morphology of the subsequent films. This is illustrated in Fig. 6, where the macroscopic roughness of the microwave-processed electrode is comparable to that of the ITO substrate—the surface appears smooth and the nanoporous nature of the film is not evident even at high SEM magnification. In comparison, Fig. 7 depicts an image of the CH electrode surface where many large and loose aggregates are visible, affording these films an increased mesoporous structure. This porous structure will result in a large specific surface area. In other words, CH electrodes have the

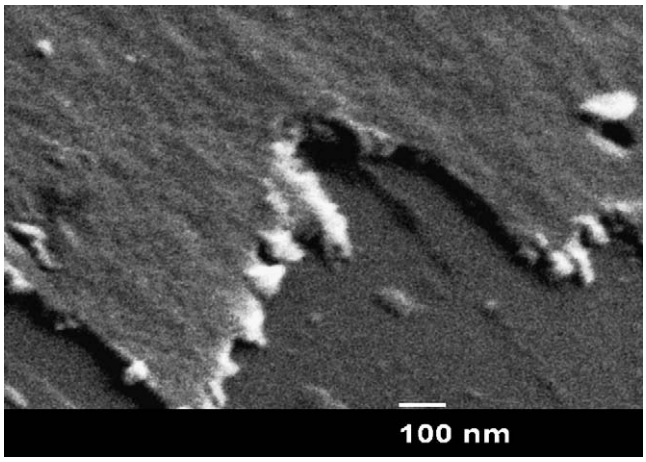

Fig. 6. SEM image of microwave-processed electrode surface (M10). Image was taken at an operating angle of 63° to the plane. The smooth macroscopic morphology of the surface is evident at this magnification.

largest overall 'effective' TiO_2 surface area for the same geometric electrode area, or in terms of oxidation capacity, have the largest number of oxidation reaction sites among all the electrodes. This also explains the behaviour of CH electrodes towards water oxidation, i.e., it has the highest background photocurrent. The increased porosity of the CH electrode would allow greater diffusion of KHP within the TiO_2 thin film. When the diffusion rate was such that oxidation of KHP was limited by the surface oxidation capacity, electrode poisoning was observed.

Another significant difference between Figs. 6 and 7 is the relative packing density of TiO_2 nanoparticles. The films produced from microwave TiO_2 (see Fig. 6) show the nanoparticles as a densely packed structure, while TiO_2 aggregates on the CH electrode are visibly loosely connected (see Fig. 7), that is, M15, M10 and M5 TiO_2 films are more compact than the CH TiO_2 film. The more compact structure of the TiO_2 film will result in more dense TiO_2 active sites for photoelectrochemical oxidation. This conclusion is supported by the HR-TEM micrographs.

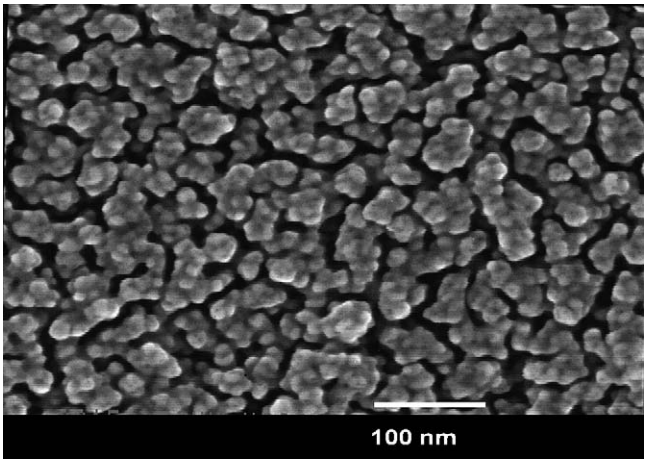

Fig. 7. SEM image of CH TiO_2 thin-film electrode. The porosity of the electrode surface is evident at this magnification in comparison to that of the microwave-treated colloidal sample of Fig. 6.

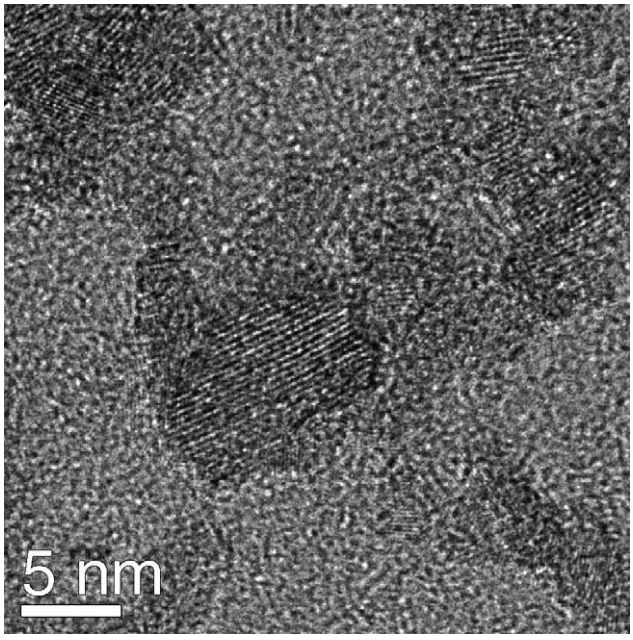

Fig. 8. High resolution-TEM micrograph of microwave-processed colloidal dispersions (M10). The spherical TiO_2 grains have an even and regular lattice appearance.

Analysis of the TiO_2 particles with HR-TEM (Fig. 8) reveals that microwave-processed colloidal particles are spherical grains of TiO_2 oriented along a single crystal plane. These spherical grains would allow for close packing within the film, leading to a dense film structure. The convection hydrothermal particles possess noticeably different crystal morphology (Fig. 9). The grain in the centre of the micrograph shows a multi-faceted crystal with no distinct epitaxial growth. The extended hydrothermal

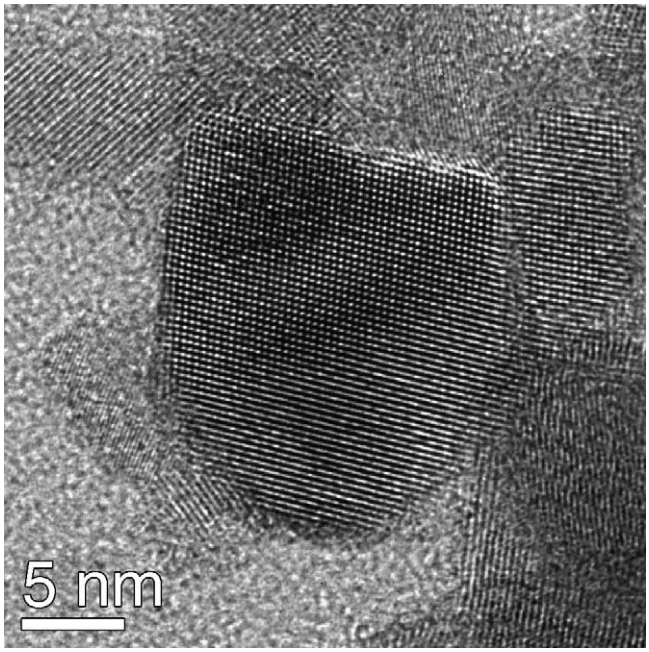

Fig. 9. High resolution-TEM micrograph of convection hydrothermal (CH) processed colloidal dispersions. The particles depicted here have multi-faceted and irregular grain morphology with disjointed lattice planes evident.

treatment results in an asymmetrical crystalline particle that, in comparison to the spherical microwave particles, would have a decreased packing density in the thin film. This discontinuously packed film gives an irregular surface morphology and increased porosity, as depicted in Fig. 7.

Poisoning occurs due to a series of factors: (i) the strong adsorption nature of KHP and its intermediates; (ii) fast mass transport of KHP; and importantly, (iii) limited oxidation capacity of the electrodes, which is related to the porosity and density of the oxidation reaction sites. In the adsorption model for KHP a bond is formed between the carboxylate groups of KHP and free Ti^{4+} atoms exposed at defect sites on the TiO_2 surface forming a much stronger pseudo titania ester linkage [30]. The incomplete oxidation of KHP also produces a chemically bound carboxylate radical. Therefore, high concentrations of KHP and/or degraded species capable of adsorption are accumulated at the electrode surface. The mechanism of oxidation of adsorbed species involves the generation of photo-holes prior to oxidation of the adsorbate; thus, any accumulation at the surface would lead to a decreased photocatalytic effect. As a result, the rate of photo-hole formation is slowed by the adsorbate, which blocks the TiO_2 electrode's reactive sites. It is reported that adsorption of KHP via carboxylate groups hinders the sites for bridged electron transfer and reactant adsorption, which will undoubtedly affect the electron transfer [31]. The increased porosity of the CH electrode apparently favours the mass transport of KHP, and increases the concentration of adsorbed carboxylate radicals, which passivates the active reaction sites. Thus at increased concentrations of KHP, the oxidation capacity of the CH electrode becomes limited compared to that of microwave-processed (M5, M10 and M15) electrodes. Hence, the nanoporous nature of microwave-processed electrodes limits diffusion within the electrode, which favours rapid exchange with the bulk solution. This effectively increases the oxidation capacity of microwave-processed electrodes for this species and mechanism of oxidation.

Overall, because of the difference in the colloidal hydrothermal treatments, M15, M10 and M5 TiO_2 electrodes have more dense reactive sites than CH TiO_2 electrodes. The surface with dense reactive sites has two advantages in terms of diminishing electrode poisoning. Firstly, less KHP and/or its intermediates can diffuse into the inner layer of the TiO_2 film and passivate reactive sites. Secondly, the efficient co-ordination among reactive sites due to the dense configuration of the reactive site can oxidise KHP and its intermediate more effectively.

This interpretation is supported by the occurrence of pale yellow stains observed on the CH TiO_2 electrode surface, which was not observed for the M5, M10 and M15 electrodes, during the photoelectrochemical oxidation of KHP. The yellow stain cannot be simply washed away but can be removed by photoelectrochemical oxidation in a supporting electrolyte solution only (i.e., without any organic compound) under UV illumination. This demonstrates that the CH TiO_2 electrodes are capable of oxidising KHP and its intermediates when the KHP concentration is low. This also indicates that the pale yellow substance on CH TiO_2 electrodes is due to the adsorption of KHP and its intermediates during the oxidation of KHP rather than the deterioration of the TiO_2 electrode. The adsorption of KHP and its intermediates occurs only when the mass transport of KHP and its intermediates are greater than the capacity of the CH electrodes. This situation does not occur for the M5, M10 and M15 electrodes because these electrodes are capable of processing KHP and its intermediates in an effective manner as discussed above.

Surface poisoning was not observed in experiments involving the oxidation of glucose with modified TiO_2 electrodes, even at a much higher concentration (up to 10 mM). This can be attributed to a number of factors. Firstly, the oxidation of KHP is more difficult than that of glucose, although complete oxidation of KHP can be achieved [2,9]. This is supported by observation of steady state oxidation currents using different TiO_2 electrodes, which were obtained at a much lower concentration for KHP (in a μM range) than that for glucose (in a mM range). Secondly, glucose, a molecule with hydroxyl functional groups, is known not to adsorb or be only weakly adsorbed to TiO_2 surfaces, thus not forming a strong chemical bond with the TiO_2 substrate. The inability to adsorb to the surface provides a more active photocatalytic environment in which the species are oxidised more readily and mass transport between the bulk and the surface occurs at an increased rate.

4. Conclusion

Among the TiO_2 thin-film electrodes examined in this study, i.e., CH, M15, M10, M5 and NP electrodes, it was demonstrated that CH TiO_2 electrodes had the highest oxidation capacity for water and glucose. However, it was also shown to be easily passivated and/or poisoned by KHP, a highly adsorptive aromatic compound. For KHP, TiO_2 electrodes prepared from microwave hydrothermal treated colloids (M15 and M10) had a higher oxidation capacity than that from CH and NP colloids, yet the surface passivation and poisoning due to excessive KHP adsorption was not observed for the M15, M10 and M5 electrodes. This can be considered as a significant advantage over CH electrodes for the photoelectrochemical oxidation of strongly adsorbed organic compounds. The affinity of the microwave samples for the oxidation of water, glucose and KHP, correlated well with their relative crystallinity as characterised by XRD and electron diffraction experiments. A change in surface and morphological properties as the polycrystalline particles assume a refined crystalline phase during the hydrothermal process can also contribute to the observed anomaly. The comparable capacity of microwave-processed electrodes for surface radical oxidation and increased photocatalytic oxidation power for adsorption-based oxidation processes demonstrate that microwave hydrothermal processing is an advantageous alternative to convection hydrothermal treatment of TiO_2 colloids.

Acknowledgments

This work was performed with the financial assistance of Griffith University Research Grant (GUNRG), AINSE Grant AINGRA04170P and facilities of the Australian Nuclear Science and Technology Organisation (ANSTO). The authors thank

the assistance of Dr. David Mitchell in the collection of high resolution-TEM micrographs and Dr. Arthur Day for SEM images of TiO_2 thin films.

References

[1] S.A. Bilmes, P. Mandelbaum, F. Alvarez, N.M. Victoria, J. Phys. Chem. B 104 (2000) 9851.
[2] H. Zhao, D. Jiang, S. Zhang, K. Catterall, R. John, Anal. Chem. 76 (2004) 155.
[3] M.C. Carotta, M. Ferroni, D. Gnani, V. Guidi, M. Merli, G. Martinelli, M.C. Casale, M. Notaro, Sens. Actuators B: Chem. 58 (1999) 310.
[4] S. Zhang, H. Zhao, D. Jiang, R. John, Anal. Chim. Acta 514 (2004) 89.
[5] B. O'Regan, M. Grätzel, Nature (London, UK) 353 (1991) 737.
[6] Y. Paz, Z. Luo, L. Rabenberg, A. Heller, J. Mater. Res. 10 (1995) 2842.
[7] R. Cinnsealach, G. Boschloo, S. Nagaraja Rao, D. Fitzmaurice, Sol. Energy Mater. Sol. Cells 57 (1999) 107.
[8] J.M. Kesselman, N.S. Lewis, M.R. Hoffmann, Environ. Sci. Technol. 31 (1997) 2298.
[9] D. Jiang, H. Zhao, S. Zhang, R. John, G.D. Will, J. Photochem. Photobiol., A. Chem. 156 (2003) 201.
[10] D. Jiang, H. Zhao, S. Zhang, R. John, J. Catal. 223 (2004) 212.
[11] C.J. Barbe, F. Arendse, P. Comte, M. Jirousek, F. Lenzmann, V. Shklover, M. Grätzel, J. Am. Ceram. Soc. 80 (1997) 3157.
[12] P.A. Venz, J.T. Kloprogge, R.L. Frost, Langmuir 16 (2000) 4962.
[13] G.J. Wilson, G.D. Will, R.L. Frost, S.A. Montgomery, J. Mater. Chem. 12 (2002) 1787.
[14] T. Schubert, M. Willert-Porada, Ceram. Trans. 111 (2001) 419.
[15] J.A. Ayllon, A.M. Peiro, L. Saadoun, E. Vigil, X. Domenech, J. Peral, J. Mater. Chem. 10 (2000) 1911.
[16] M. Zhou, W.Y. Lin, N.R. de Tacconi, K. Rajeshwar, J. Electroanal. Chem. 402 (1996) 221.
[17] M.E. Calvo, R.J. Candal, S.A. Bilmes, Environ. Sci. Technol. 35 (2001) 4132.
[18] K. Vinodgopal, S. Hotchandani, P.V. Kamat, J. Phys. Chem. 97 (1993) 9040.
[19] D. Tafalla, P. Salvador, J. Electroanal. Chem. Interfacial Electrochem. 270 (1989) 285.
[20] S.U.M. Khan, T. Sultana, Sol. Energy Mater. Sol. Cells 76 (2003) 211–221.
[21] J.A. Byrne, B.R. Eggins, W. Byers, N.M.D. Brown, Appl. Catal. B: Environ. 20 (1999) L85.
[22] S. Horikoshi, Y. Satou, H. Hidaka, N. Serpone, J. Photochem. Photobiol. A. Chem. 146 (2001) 109.
[23] M. Takahashi, K. Tsukigi, T. Uchino, T. Yoko, Thin Solid Films 388 (2001) 231–236.
[24] D.F. Ollis, H. Al-Ekabi, Photocatalytic purification and treatment of water and air: Proceedings of the first International Conference on TiO_2 Photocatalytic Purification and Treatment of Water and Air, London, Ontario, Canada, 8–13 November 1992, in: Trace Metals in the Environment, vol. 3, Elsevier, Amsterdam/New York, 1993.
[25] K. Vinodgopal, U. Stafford, K.A. Gray, P.V. Kamat, J. Phys. Chem. 98 (1994) 6797.
[26] A. Fujishima, T. Inoue, K. Honda, J. Am. Chem. Soc. 101 (1979) 5582.
[27] J.A. Byrne, B.R. Eggins, J. Electroanal. Chem. 457 (1998) 61.
[28] M.R. St. John, A.J. Furgala, A.F. Sammells, J. Phys. Chem. 87 (1983) 801–805.
[29] E. Skou, Electrochim. Acta 22 (1977) 313.
[30] N.W. Duffy, K.D. Dobson, K.C. Gordon, B.H. Robinson, A.J. McQuillan, Chem. Phys. Lett. 266 (1997) 451.
[31] S.R. Morrison, Electrochemistry at Semiconductor and Oxidized Metal Electrodes, Plenum Press, New York, 1980.